Incorporating stimulus-responsive character into filamentous virus assemblies

Harry Bermudez* and Adam P. Hathorne

Received 14th January 2008, Accepted 31st January 2008
First published as an Advance Article on the web 30th April 2008
DOI: 10.1039/b800675j

Controlling interactions between building blocks, in either guided- or self-assemblies, is becoming increasingly important for the creation of functional materials. We have focused our attention on the well-known model assembly, the filamentous bacteriophage, where our strategy is to selectively alter surface features by focusing on spatially distinct capsid proteins. Towards introducing stimulus-responsive behavior in these flexible, rod-like particles, we have introduced elastin-like polypeptide (ELP) motifs of isoleucine and tyrosine "guest" residues by recombinant DNA methods. Our hypothesis is that modification of the major coat capsid protein would be greatly amplified by the 2700 copies per particle. Characterization of ELP-phage particles was carried out by microbiological assays, zeta potential, dynamic light scattering, and calorimetry. Bacteria producing ELP-phage particles grow more slowly and surprisingly, ELP-modified phages display a significant reduction in viral infectivity. For the lengths of ELP inserts studied, modified phages do not aggregate from solution as monitored by DLS. However, the hydrodynamic size of the phages depends on the details of the ELP motif. Zeta potential measurements reveal the particles are electrostatically stabilized, and this contributes in part to the energetic barrier against aggregation. Preliminary calorimetric data indicate subtle thermal transitions in the range 35–45 °C, suggesting that the ELP motif may collapse without triggering macroscopic aggregation. The results are consistent with the classical picture of critical solution phenomena at low concentrations, where to drive phase separation, solvent quality must be increasingly poor. Apart from being model systems to study basic questions of self-assembly, extending these modular systems is likely to result in improved understanding and control over self-assembly in various applications.

Introduction

Self-assembly in solution relies not only on thermodynamic and kinetic factors but on the directionality of interactions. It is this directionality that distinguishes useful "assembly" from undesirable "aggregation". Well-known assemblies such as micelles and vesicles are symmetric largely due to the weak directional nature of hydrogen bonding (the hydrophobic effect) that drives their formation in water. Additional types of long-range interactions lead to more complex structures, accounting for the vast difference between an idealized collapsed polymer globule and a folded functional protein. Yet in spite of that difference, theoretical

Department of Polymer Science & Engineering, University of Massachusetts, Amherst, MA 01003, USA. E-mail: bermudez@polysci.umass.edu; Fax: +1 413 545 0082; Tel: +1 413 577 1413

developments such as lattice models have greatly improved our understanding of protein folding and stability.[1] It becomes clear that objects with high degrees of symmetry have limited functionality and thus there is an increased effort towards the creation of asymmetric assemblies.[2–4]

Asymmetry is relevant at multiple length scales in biology, from the molecular-level orientation of transmembrane proteins to the tissue level where it is essential to development. To the materials scientist, the tools of protein engineering combined with relatively simple biological model systems provide opportunities to establish design criteria for creating new asymmetric assemblies. One such widely-known model system is the filamentous bacteriophage.[5] Indeed, phages as a family provided the foundation of molecular biology[6,7] and their numerous members are now finding diverse applications.[8–12] The protein capsid of the M13 filamentous bacteriophage consists of only five types of structural proteins,[13] allowing the use of molecular biology to tailor these viruses with a degree of precision that is difficult to achieve with traditional inorganic particles. The major capsid protein, also known as pVIII, is present in approximately 2700 copies per phage and thus makes up the majority of the surface (Fig. 1). The minor coat protein pIII has a far smaller copy number of only five, yet it plays a key role in viral infectivity. This natural decoupling of spatial location and function inherent in the viral capsid suggests an approach to alter bacteriophage properties by manipulating specific capsid proteins (Fig. 1).

Apart from their role in virology, phages can be used to explore fundamental questions of self-assembly in the context of the capsid. Such viruses can also be thought of as tunable colloids or nanoscale scaffolds.[14,15] Control over placement of reactive groups on virus particles such as phages has been clearly demonstrated,[16,17] but responsiveness to environmental stimuli is still lacking. As a step in this direction we have used recombinant DNA techniques to display elastin-like polypeptides (ELPs) on the surface of filamentous bacteriophage particles. The thermoresponsive character of elastin-like polypeptides varies with the length and composition of the genetically encoded monomeric unit: $(VPGXG)_n$ where X denotes any amino acid but proline.[18] The molecular description of the ELP transition is still unclear, but it is generally believed to be explained by increasingly poor hydration of the polypeptide, leading to intramolecular beta-type interactions.[19,20] Nevertheless, ELPs have found numerous applications exploiting their switching behavior, ranging from the macroscopic to the single-molecule level.[21–25] Due to the inverse dependence of transition temperature T_t with chain length,[26] we have focused our attention on short segments with $n = 1,3,6$ where hydrophobic residues are placed in the "guest"

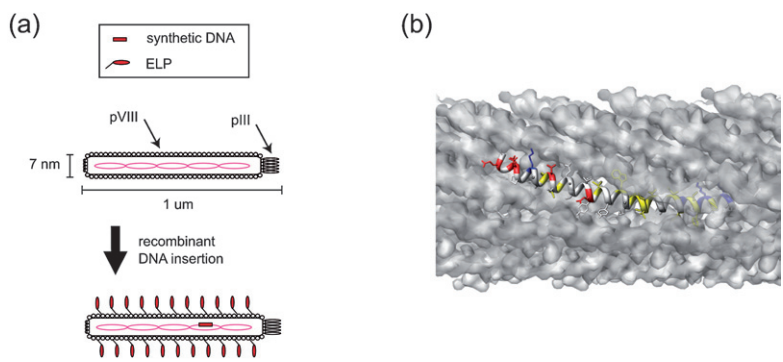

Fig. 1 (a) Schematic of filamentous bacteriophage structure, depicting the major (pVIII) and minor (pIII) coat proteins; the remaining three types of structural proteins are not shown. Recombinant DNA insertion leads to displayed peptides on each copy of the corresponding capsid protein. (b) Section of a multimolecular model (PDB ID: 1IFJ) of the phage capsid showing alpha-helical nature of pVIII and the staggered orientation of the many pVIII proteins. One copy of pVIII is highlighted for clarity.

position. In principle, by varying the guest residue and/or chain length, the responsive behavior could be modulated with a high degree of control.

Experimental

ELP fusion construction

Synthetic oligonucleotides containing the ELP sequence were designed and purchased from Integrated DNA Technologies. To form appropriate overhangs for ligation, four to six oligos were annealed from 95 to 15 °C at a rate of −1 °C min^{-1} to generate the double-stranded insert. The 5′-ends of the insert were subsequently phosphorylated with T4 polynucleotide kinase. The M13KO7 phage vector (Amersham) was digested at two sites with the restriction enzyme BbvCI, gel purified and extracted (Qiagen). Vector and insert were ligated with T4 DNA ligase at a 3 : 1 insert–vector ratio. Subsequent transformation of the plasmid into either DH5a (Invitrogen) or TG1 (Biochain) *E. coli* competent cells was performed according to standard techniques. Positive selection for transformants was achieved by use of kanamycin resistance. All enzymes were purchased from New England Biolabs.

To screen clones for ELP insertion, plasmid DNA was isolated from single colony cultures using a Qiaprep Spin Miniprep Kit (Qiagen). Plasmid concentrations were measured using a Nanodrop ND-1000 spectrophotometer. PCR screening primers, flanking and straddling the insert region, were designed and purchased (IDT) and used to amplify desired target regions. PCR products were visualized on a 1.2% agarose gel to identify positive inserts. Upon PCR confirmation of the insert, plasmid DNA was sequenced by GeneWiz with the upstream primer 5′-AGGTTGGTGCCTTCGTAG-3′ to ensure no errors were present.

Phage isolation

Large-scale cultures of 200–250 mL 2xYT media (Teknova) with 15 μg mL^{-1} kanamycin were grown from single colonies of each respective ELP clone. After centrifuging the cultures for 30 minutes at 3000 g to remove bacterial cells, the supernatant was collected and 0.15 vol PEG-8000–NaCl solution (25%w/v, 2 M) added. Solutions were gently mixed and incubated at 4 °C for 3 h, followed by centrifugation at 3100 g for 80 min to pellet the phages. The supernatant was removed and 20–30 mL of 1× PBS added to resuspend the phage pellet. The solution was centrifuged at 10 000 g for 10 min to clear the supernatant and a second precipitation was performed by adding 0.15 vol. PEG-8000–NaCl to the supernatant, followed by incubation at 4 °C overnight. The phages were re-pelleted by centrifugation at 15 000 g for 40 min. After removal of the supernatant, the phage pellet was resuspended in 5 mL of 1× PBS by gently shaking at room temperature. Solutions were spun one final time at 10 000 g for 10 min to remove any remaining debris and the supernatant stored at 4 °C. Unless otherwise specified, reagents were purchased from Sigma-Aldrich and Fisher Scientific.

Characterization

Analysis of the ELP-phage behavior was performed using microbiological assays, dynamic light scattering, zeta potential, and calorimetry. Growth curves were developed for bacteria harboring each ELP in order to determine whether the incorporation of the ELP into the pVIII protein had any impact on host growth rate. The optical density at 600 nm of bacterial cultures was monitored using a Nanodrop ND-1000 spectrophotometer. Time constants were calculated based on semi-log plots of absorbance *versus* time. Viral infectivity, also known titering, was determined by mixing known dilutions of phage solutions with uninfected TG1 *E. coli* bacteria and incubating for 30 min at 37 °C. Spots of the mixture were subsequently

applied onto LB agar plates with 40 μg mL^{-1} kanamycin and incubated overnight to allow colony formation.

A Nano-ZS Nanoseries Zetasizer (Malvern Instruments) was used to examine hydrodynamic size and zeta potential. Approximately 400–500 μL of phage solutions were loaded into PMMA low volume disposable cuvettes. Temperature scans were conducted from 5 to 75 °C with an interval 10–15 °C and a 2 min equilibration time. In order to determine if deprotonation of the tyrosine guest residue would result in a shift of the transition temperature, the pH of the phage solutions was adjusted using 0.1–1 M NaOH. Zeta potential measurements were conducted at 25 °C using disposable capillary cuvettes (Malvern).

Calorimetric data was acquired with a TA Instruments Q1000 differential scanning calorimeter. Approximately 20–25 mg of sample was loaded into a aluminium chamber and hermetically sealed. Samples were heated and cooled at a rate of 10 °C min^{-1} from 20–70 °C, using air as a reference.

Results and discussion

ELP fusion design

Gene VIII, which encodes the major coat protein (pVIII), contains two BbvCI restriction sites. The first site cuts at DNA encoding for the alanine residue A1 at the amino terminus of the mature protein, and the second site after A16. Thus, to properly construct the ELP fusion required re-introducing approximately 50 bp of DNA encoding residues 2–16 (see Table 1). In that process we performed silent mutations in the mentioned region to enhance the codon preference of *E. coli*: specifically, Pro (CCC to CCG), Ala (GCN to GCT), Phe (TTT to TTC).

The position of the first BbvCI site is additionally useful because of the proximity to the amino terminus of pVIII, and hence fusions at that position are likely to be solvent-accessible rather than buried in the capsid interior. Indeed, it is known that single cysteines on phage capsids display sequence/position dependent reactivity.[27] Also important is preserving the ability of the modified protein pVIII to properly self-assemble in the bacterial cell membrane, a process still poorly-understood[13] but known to involve both electrostatic interactions near the carboxy terminus and hydrophobic residues in the center of pVIII.

The ELP clones are named according to the guest residue X and number of repeats, *n*: for example $(VPGYG)_3$ is denoted as Y_3. Because of the inverse dependence of transition temperature T_t with chain length,[26] increases in T_t at short chain lengths would be presumably offset by the low "asymptotic" $T_{t,\infty}$ at very long chain lengths ($n > 150$). Thus isoleucine and tyrosine were chosen as guest residues, having asymptotic $T_{t,\infty}$ of 10 and −55 °C, respectively. There has been limited investigation

Table 1 DNA and amino acid sequence of the phage major coat protein pVIII (residues 1–17).

M13KO7[a]	↓ GCT GAG GGT GAC GAT CCC GCA AAA GCG GCC TTT AAC TCC A E G D D P A K A A F N S ↓ CTG CAA GCC TCA ... L Q A S ...
ELP constructs[b]	GCT GAG GTT CCG GGT XXX GGT GGT GAC GAC CCG GCT AAA A E **V** **P** **G** **X** **G** G D D P A K GCT GCT TTC AAC TCC CTG CAA GCT TCA ... A A F N S L Q A S ...

[a] Arrows denote BbvCI sites. [b] X is the "guest" residue in the ELP motif, in this study either tyrosine (Y) or isoleucine (I).

of relatively short ELP sequences, with a few notable exceptions. For example, Reiersen and coworkers[28] used solid-phase peptide synthesis and circular dichroism to examine short versions of the classical $(VPGVG)_n$ motif where $n = 1,3,5$. In contrast to the predictions of both Urry and Chilkoti, they found T_t to range from 21–41 °C at pH 7. This is a rather modest change given that the asymptotic $T_{t,\infty}$ for valine is 21 °C, and even more surprising when compared to the predicted[26] $T_t = 163$ °C for $n = 5$. It must be pointed out that such small ELPs might undergo structural transitions yet not exhibit sufficient hydrophobicity to drive aggregation of the much larger particles in dilute solutions.

In our ELP-phage solutions, the ELP concentration does not exceed 5 μM, in spite of the high copy number of pVIII on phage particles. However, as the ELP is essentially "grafted" to each pVIII, the local concentration is effectively that of a brush with a density of 2700 copies per particle surface area. Taking the brush length as the ELP contour length gives a minimum local concentration of 170 μM for $n = 1$, down to 28 μM for $n = 6$; a significant enhancement compared to the "bulk" concentration. Even so, at low concentrations and short chain lengths, there is still evidence for ELP functionality. For example, in two separate cases of ELP linkers, thermoresponsive binding effects were observed with as little as a single repeat ELP unit.[25,29]

Apart from the thermoresponsive behavior of ELP motifs, certain amino acids have inherent characteristics which might be additionally exploited. For example, tyrosine has a pK_a of 10.1, and when deprotonated has an asymptotic $T_{t,\infty} = 120$ °C; thus for short ELP sequences, T_t should be elevated even higher, making it effectively inaccessible. Therefore by changing the pH of the phage environment, the tyrosine ELP clones (Y_1,Y_3,Y_6) should exhibit a pH-dependent transition above the pK_a.

Growth of infected *E. coli* and infectivity of ELP-phages

One of our concerns was that upon synthesis, the hydrophobic ELP-modified pVIII proteins would cause intracellular aggregation, leading to growth inhibition or even death of the host bacteria before significant amounts of virus could be produced. To check for this possibility, we monitored the optical density at 600 nm through the exponential phase for all constructs. The time constants measured are all either slower or equal in growth compared to its M13KO7 counterpart (Fig. 2a). This result suggests the transition temperature is near 37 °C, or that intracellular levels

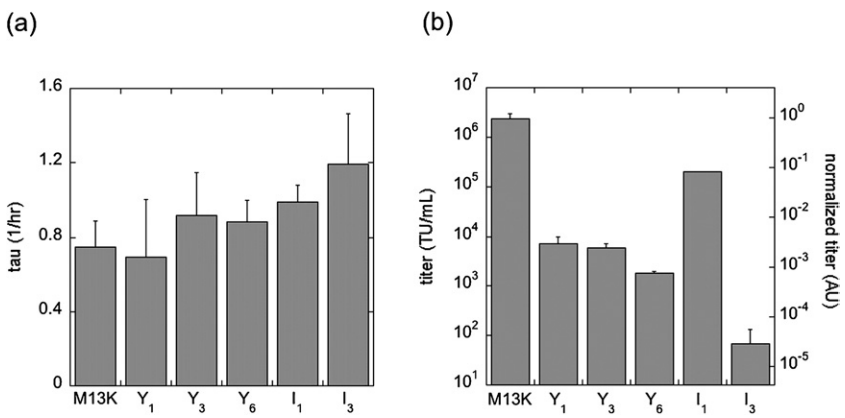

Fig. 2 (a) Time constants for TG1 *E. coli* bacteria infected with ELP-phage DNA. Note that ELP-phage particles are secreted throughout bacterial growth. In general, longer ELP inserts result in slower growth as compared to the parental M13KO7. (b) Infectivity of ELP-phages determined by titering. Here, longer ELP inserts on phages lead to a reduced ability to infect bacteria.

of the ELP-modified pVIII begins to accumulate to inhibitory concentrations, although this would be mitigated by active secretion of virus particles. In spite of the slower growth, virus particles are still produced in comparable numbers by the infected bacteria (data not shown). It is well-known that virus production diverts energy and resources from the natural growth of the bacteria, and it may be even more so in the case of a larger and more hydrophobic capsid building block. Interestingly, our unsuccessful attempts to construct an I_6 ELP-phage are consistent with these results. In this case, if the growth inhibition is solely due to effects of intracellular I_6 ELP-pVIII levels, incubation at lower temperatures may circumvent this problem.

The ability of ELP-phage particles to infect *E. coli* is substantially reduced due to the presence of the ELP, except for I_1 (Fig. 2b). Such a result is intriguing, given that infectivity is mediated by the minor coat protein (pIII) on the viral capsid binding to the bacterial coat protein pilin and not the pVIII protein where the ELP is displayed.[13] However, the titering assay cannot discriminate among any of the events involved in infection: phage–bacteria binding, DNA insertion, DNA replication, protein synthesis, and secretion. As seen in Fig. 2a, once the phage DNA is internalized, bacterial growth is negatively impacted. Inhibition of any one or several of the remaining steps needed to complete the phage "life cycle" could explain the results in Fig. 2b. Over the course of several weeks, a gradual decrease in infectivity was also observed (data not shown), indicating a role for non-specific interactions among phage particles or structural changes in the capsid. Regardless of the mechanism, this would further reduce the availability of phage particles binding to bacteria, leading to lower overall infectivity.

Dynamic light scattering

Diffusion of phage particles in a dilute solution potentially gives insight into particle–particle aggregation among ELP-phages. To minimize particle–particle effects before reaching the desired transition temperature, all samples were measured at or below a concentration of approximately $c = 1 \times 10^{12}$ virus per mL or 30 μg mL^{-1}, which is below the overlap[30] concentration c^*=1 particle per length^3 = 2×10^{12} virus per mL. Due to the rod-like shape of the viral particles, the average translational diffusion coefficent D has unequal contributions from diffusion along the rod axis and the other two orthogonal directions. Nevertheless an "equivalent" hydrodynamic sphere size can be determined and is useful as a first approximation. Above the transition temperature, we initially expected the increased hydrophobicity to drive attractive interactions leading to aggregation and, perhaps, precipitation.

Over the temperature range 5–75 °C, the were no significant changes in the z-average size, indicating a lack of particle aggregation. The presentation of the ELP motif on pVIII will increase the diameter of phages, yet surprisingly, $Y_3 > Y_1 > Y_6$, suggesting that the Y_6 ELP-phage may be somewhat collapsed on the capsid surface. Conversely, Y_3 may be unusually extended away from the capsid surface. The lack of aggregation can perhaps be best understood in the context of critical solution phenomena, where as first recognized by Flory,[31] low concentrations require that the solvent quality become increasingly "poor" to drive phase separation. Such changes in solvent quality could be achieved by either using more hydrophobic guest residues, such as tryptophan, or by adding chaotropes such as urea.

Zeta potential

The major coat protein pVIII possesses acidic residues near its amino terminus and thus the particles are electrostatically stabilized in solution (see Table 1). We surmised that the presence of an ELP insertion (NH_2-AE↓GDD…) at or near the terminus would alter the effective charge on the phage capsid. Measurements of

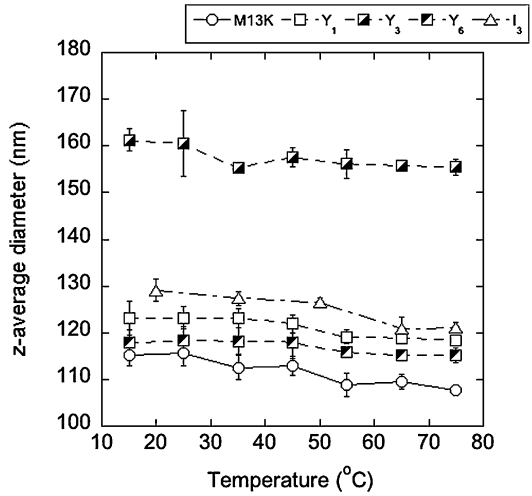

Fig. 3 Average hydrodynamic size of ELP-phages as determined by dynamic light scattering.

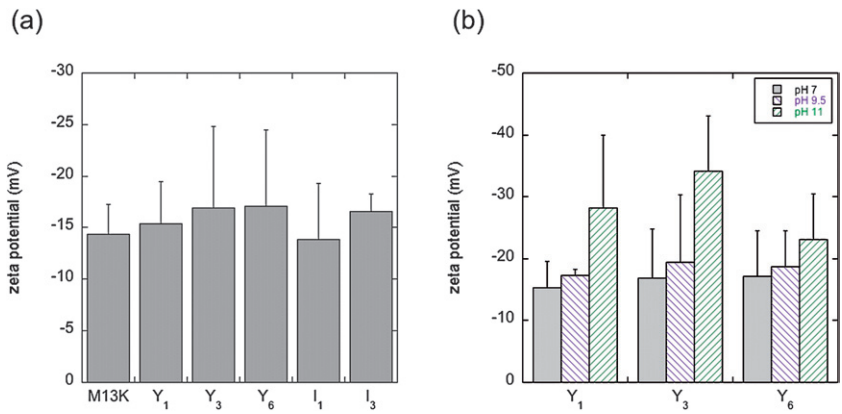

Fig. 4 (a) Zeta potential of ELP-phages in 1.5 mM NaCl at pH 7, 25 °C. (b) Dependence of zeta potential on pH for tyrosine ELP-phages.

the zeta potential at low ionic strength (1.5 mM NaCl, pH 7) showed little to no change in surface charge between ELP-modified particles and the parental M13KO7 phage (Fig. 4). This may be due to the ELP motif having predominantly small side-chains, while also being largely ordered and extended below T_t. Presumably, above T_t the zeta potential will be reduced by collapse of the ELP chain towards the surface. This effect would be most pronounced for Y_3, with the largest apparent hydrodynamic size. At higher pH, as expected, the zeta potential increases for all the tyrosine phages. Here the smallest effect appears to be for Y_6, which in view of the DLS results (Fig. 3), suggests that the more compact physical conformation of the ELP motif may attenuate the increase in surface charge. Of course, the inherent surface charge of the phages provides a barrier to aggregation that is not present for soluble ELP polymers. Site-directed mutagenesis of charged residues in pVIII would directly reveal their role in counteracting aggregation above T_t.

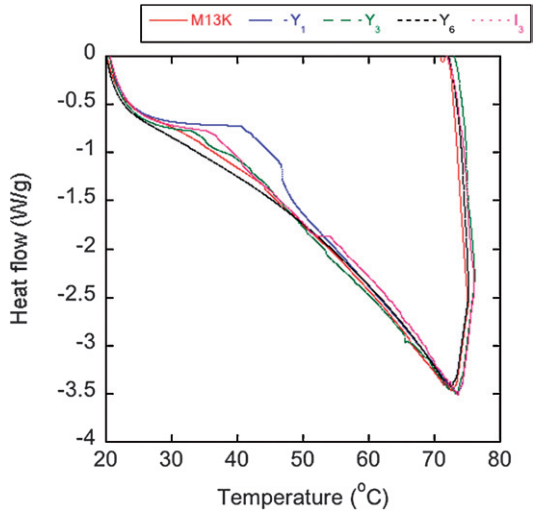

Fig. 5 Differential scanning calorimetry of ELP-phages as compared to the parental M13KO7 phage. Scans were conducted from 20–80 °C at a rate of 10 °C min^{-1}.

Calorimetry

The absence of micro- and macroscopic aggregation is consistent with the picture of a lower critical solution phenomena at dilute concentrations. Nevertheless, the ELP motif can still undergo structural changes from an open beta-spiral to a disordered compact chain upon exceeding T_t. Preliminary calorimetry experiments reveal for both tyrosine and isoleucine ELP-phages, subtle differences in the heating curves can be observed when compared to M13KO7, between 35–45 °C (Fig. 5). While speculative at this stage, it does appear that shorter tyrosine motifs exhibit higher transition temperatures. The minimum near 75 °C is an artifact from the range of the heating cycle runs, but in any case protein denaturation of the phage proteins would be likely to occur by this point.

Summary

The filamentous bacteriophage capsid provides a platform for introducing novel functionality in the form of displayed polypeptides. Stimulus-responsive polypeptides, such as the ELP motif, are capable of conferring tunable properties to their phage scaffolds. This work is a first attempt to incorporate dynamic control over phage properties such as size and charge—potentially enabling new applications for these materials. In contrast to large ELP polymers that aggregate above their T_t, it seems clear that much shorter ELP chains grafted to phage particles will remain in solution unless they are sufficiently hydrophobic. However, given that the ELP motif can still switch between an extended to collapsed state implies the ability for capture/release of small molecules.

Further characterization at the protein level using techniques such as circular dichroism should reveal if the ELP motif alters the largely alpha-helical nature of the major coat protein (pVIII). Together with electron/scanning probe microscopies, structural changes in the phage capsid—possibly manifested as changes in preferred curvature or bending stiffness—should also be apparent. Other, more hydrophobic, guest residues such as tryptophan might be capable of inducing aggregation, yet phage production in bacteria may also be more strongly inhibited. Combination of ELP motifs with additional functionality in phage capsids, such as the streptavidin-binding tripeptide HPQ, might allow for the

creation of directed phage-based networks with the ELP acting as a stimulus-responsive linker.

Acknowledgements

The authors thank Sam Pendergraph for initial design contributions to this work and H. Henning Winter for use of his calorimeter. Support from the Materials Research Science and Engineering Center (MRSEC, DMR-0213695) and the Nanoscale Science and Engineering Center (NSEC, CMMI-0531171) at the University of Massachusetts Amherst is gratefully acknowledged.

References

1 K. A. Dill, D. O. Alonso and K. Hutchinson, *Biochemistry*, 1989, **28**, 5439–5449.
2 C. L. Cheung, S. W. Chung, A. Chatterji, T. W. Lin, J. E. Johnson, S. Hok, J. Perkins and J. J. De Yoreo, *J. Am. Chem. Soc.*, 2006, **128**, 10801–10807.
3 R. Stoenescu and W. Meier, *Chem. Commun.*, 2002, 3016–3017.
4 Q. Wang, T. Lin, J. E. Johnson and M. G. Finn, *Chem. Biol.*, 2002, **9**, 813–819.
5 Z. Dogic and S. Fraden, *Phys. Rev. Lett.*, 1997, **78**, 2417–2420.
6 F. H. Crick and J. D. Watson, *Nature*, 1956, **177**, 473–475.
7 J. B. Bancroft and P. Kaesberg, *Nature*, 1958, **181**, 720–721.
8 D. Prasuhn, R. M. Yeh, A. Obenaus, M. Manchester and M. G. Finn, *Chem. Commun.*, 2007, 1269–1271.
9 P. A. Suci, D. L. Berglund, L. Liepold, S. Brumfield, B. Pitts, W. Davison, L. Oltrogge, K. O. Hoyt, S. Codd, P. S. Stewart, M. Young and T. Douglas, *Chem. Biol.*, 2007, **14**, 387–398.
10 P. J. Yoo, K. T. Nam, J. Qi, S.-K. Lee, J. Park, A. M. Belcher and P. T. Hammond, *Nat. Mater.*, 2006, **5**, 234–240.
11 K. T. Nam, B. R. Peelle, S. W. Lee and A. M. Belcher, *Nano Lett.*, 2004, **4**, 23–27.
12 C. B. Mao, D. J. Solis, B. D. Reiss, S. T. Kottmann, R. Y. Sweeney, A. Hayhurst, G. Georgiou, B. Iverson and A. M. Belcher, *Science*, 2004, **303**, 213–217.
13 D. A. Marvin, *Curr. Opin. Struct. Biol.*, 1998, **8**, 150–158.
14 C. M. Soto, A. S. Blum, G. J. Vora, N. Lebedev, C. E. Meador, A. P. Won, A. Chatterji, J. E. Johnson and B. R. Ratna, *J. Am. Chem. Soc.*, 2006, **128**, 5184–5189.
15 M. Uchida, M. T. Klem, M. Allen, P. Suci, M. Flenniken, E. Gillitzer, Z. Varpness, L. O. Liepold, M. Young and T. Douglas, *Adv. Mater.*, 2007, **19**, 1025–1042.
16 E. Gillitzer, P. Suci, M. Young and T. Douglas, *Small*, 2006, **2**, 962–966.
17 Q. Wang, T. Lin, L. Tang, J. E. Johnson and M. G. Finn, *Angew. Chem., Int. Ed.*, 2002, **41**, 459–462.
18 D. W. Urry, *J. Phys. Chem. B*, 1997, **101**, 11007–11028.
19 B. Li, D. O. V. Alonso and V. Daggett, *J. Mol. Biol.*, 2001, **305**, 581–592.
20 C. M. Venkatachalam and D. W. Urry, *Macromolecules*, 1981, **14**, 1225–1229.
21 S. C. Heilshorn, J. C. Liu and D. A. Tirrell, *Biomacromolecules*, 2005, **6**, 318–323.
22 J. Hyun, W.-K. Lee, N. Nath, A. Chilkoti and S. Zauscher, *J. Am. Chem. Soc.*, 2004, **126**, 7330–7335.
23 D. E. Meyer and A. Chilkoti, *Nat. Biotechnol.*, 1999, **17**, 1112–1115.
24 Z. Megeed, R. M. Winters and M. L. Yarmush, *Biomacromolecules*, 2006, **7**, 999–1004.
25 H. Reiersen and A. R. Rees, *Biochemistry*, 1999, **38**, 14897–14905.
26 D. E. Meyer and A. Chilkoti, *Biomacromolecules*, 2004, **5**, 846–851.
27 H. Bermudez, , S. Kontos and and J. A. Hubbell, , 2007, in preparation.
28 H. Reiersen, A. R. Clarke and A. R. Rees, *J. Mol. Biol.*, 1998, **283**, 255–264.
29 Z. Megeed, R. M. Winters and M. L. Yarmush, *Biomacromolecules*, 2006, **7**, 999–1004.
30 S. Schulz, E. Maier and R. Weber, *J. Chem. Phys.*, 1989, **90**, 7–10.
31 P. J. Flory, *J. Chem. Phys.*, 1941, **9**, 660–661.